International Round-Robin Tests on Solar Cell Degradation Due to Electrostatic Discharge

International Round-Robin Tests on Solar Cell Degradation Due to Electrostatic Discharge

Teppei Okumura*
Japan Aerospace Exploration Agency, Tsukuba 305-8505, Japan

Mengu Cho†
Kyushu Institute of Technology, Kitakyushu 804-8550, Japan

Virginie Inguimbert‡
ONERA, 31055 Toulouse, France

Denis Payan§
Centre National d'Etudes Spatiales, 31401 Toulouse, France

Boris Vayner¶
Ohio Aerospace Institute, Cleveland, Ohio 44142

and

Dale C. Ferguson**
U.S. Air Force Research Laboratory, Albuquerque, New Mexico

DOI: 10.2514/1.47929

Primary discharge occurs on solar arrays due to their interaction with the space plasma. A solar cell may suffer degradation of electrical performance if the primary discharge occurs at the cell edge. To estimate the power generated at the end of life, it is necessary to study the details of solar cell degradation. However, throughout the world, primary discharge has not been recognized as a cause of solar cell degradation. There is now an international collaboration among institutions in Japan, France, and the United States toward a common international standardization of solar array electrostatic discharge test methods. Round-robin tests were carried out as part of this collaborative research. Laboratory experiments were performed at the same time in three institutions using the same test method and identical solar cells. Solar cell degradation was confirmed at all three institutions. It was found that a multijunction solar cell is more susceptible to damage from primary discharge than a crystalline silicon solar cell. Throughout the round-robin tests, discharge has been shown to be a significant cause of solar cell degradation.

Nomenclature

C_{ext}	=	external capacitance, F
C_p	=	current probe
C_{sat}	=	capacitance of the satellite, F
dP_{max}	=	variation of P_{max} per primary discharge, W
dI_{leak}	=	variation of I_{leak} per primary discharge, A
I_0	=	inverted saturation current, A
I_{leak}	=	leak current of solar cell, A
I_{peak}	=	peak of primary discharge, A
I_{sc}	=	short circuit current, A
N_{arc}	=	number of primary discharge
P_{max}	=	maximum power, W
Q_{arc}	=	primary discharge charge, Q
R_s	=	series resistance of solar cell, Ω
R_{sh}	=	parallel resistance of solar cell, Ω
T_{arc}	=	primary discharge duration, s
T_{i1}, T_{i2}	=	start and end times of primary discharge current, s
T_{p1}, T_{p2}	=	start and end times of primary discharge power, s
V_b	=	voltage power supply, V
V_{oc}	=	open circuit voltage, V
V_p	=	voltage probe
W_{arc}	=	primary discharge energy, J

I. Introduction

THE primary discharge (trigger arc, primary arc) on the solar array has been studied for years. When primary discharge occurs on a solar cell, the material of the solar cell melts as the current concentrates at the cathode spot of a primary discharge. Therefore, the solar cell can potentially suffer degradation due to the primary discharge. Toyoda et al. first found solar cell degradation due to a primary discharge in ground discharge experiments [1,2]. Okumura et al. [3] presented an extensive study of the solar cell degradation. Figure 1 shows a discharge track leading to solar cell degradation. In this case, the cathode spot is generated at the edge of the solar cell, and then the primary discharge reaches the surface electrode. When the discharge track shown in Fig. 1 shorts the surface electrode and the back surface electrode (or the P layer) of the solar cell, the electrical performance of the solar cell decreases. Based on a microscopic picture of the back surface shown in Fig. 1, the size of the discharge track is $100 \times 30\ \mu m^2$; hence, the size of the cathode spot could be smaller. Therefore, heat injected to an area of $3 \times 10^{-9}\ m^2$ led to the observed solar cell degradation. In contrast, a primary discharge that occurs at the bus bar or on the interconnector does not cause solar cell degradation [4]. The reason is that the primary discharge does not directly inject heat into the solar cell material. A primary discharge at the bus bar or the interconnector may cause degradation of the bypass diode of the solar cell, because the primary discharge current generates a voltage surge on the solar cell [5]. Because degradation due to the voltage surge is not the same
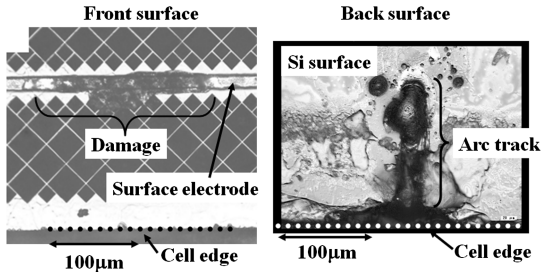
Fig. 1 Discharge track on Si cell.

as the degradation due to the primary discharge, this phenomenon is not considered further in this paper. In [5], the degradation due to voltage surges is discussed in detail.

In the space environment, radiation is well known for its severely degrading effects on solar cell performance [6]. Therefore, the size of the solar array is mainly determined by the spacecraft power requirements and the electrical performance at the end of its lifetime. Because degradation of solar cells is due not only to radiation effects but also to primary discharge, solar cell degradation due to the primary discharge may need to be taken into account in estimating the electrical performance at the end of life. To help predict solar cell degradation in orbit, the solar cell degradation must be characterized via ground tests, while changing the primary discharge parameters, such as peak current, pulse duration, energy, etc.

In the present research project aimed at standardizing solar array electrostatic discharge (ESD) tests, solar cell degradation due to primary discharge is recognized as a significant issue [7]. Unlike solar cell degradation due to radiation, the degradation due to discharge has generally not been recognized throughout the world. Therefore, there was a need to experiment in different experimental facilities in different countries using identical discharge circuits and solar cells to show that the degradation due to primary discharges is real. Okumura et al. [8], Mateo-Velez et al. [9], and Vayner et al. [10] independently reported some of the experiment results found in France, the United States, and Japan, in which a round-robin test was carried out using identical test samples and experimental circuits. The purpose of the present paper is to add new results and to summarize the experimental data for archival purpose. In Sec. II, the samples and the differences among the experimental facilities are discussed. The differences between the primary discharge current waveforms recorded in various laboratories were carefully investigated. In Sec. III, the degradation of InGaP/GaAs/Ge solar cells (multijuction, or MJ, cells) is discussed. The degradation threshold of MJ cells for several primary discharge parameters are determined, such as peak current, pulse duration, and energy. In Sec. IV, the degradation of silicon solar cells (Si cells) is discussed.

II. Experiment

A. Experimental Samples

Figure 2 shows the experimental samples. Three types of solar cells were prepared: a silicon solar cell with an integrated bypass function (IBF), a silicon solar cell without an integrated bypass function, and an MJ cell. Because the exterior appearance of the Si without IBF cell is exactly the same as the Si with IBF cell, the Si without IBF cell is omitted from Fig. 2. The size of the Si with and without IBF cell is 35×70 mm^2. The size of the MJ cell is 40×70 mm^2. Each solar cell is glued to the polyimide film on
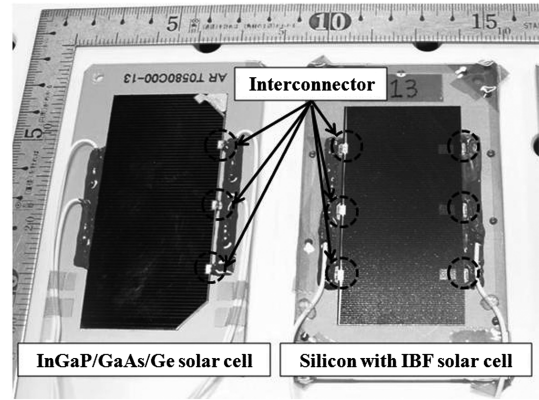

Fig. 2 Experimental samples: InGaP/GaAs/Ge solar cell and silicon with IBF solar cell.
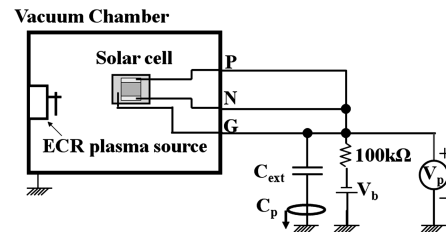

Fig. 3 Discharge circuit.

aluminum plate. A cover glass is attached to the top of the solar cell with a transparent adhesive. The electrical performances of all the solar cells were measured and confirmed to comply with flight quality requirements. Table 1 shows the initial value of the short circuit current, I_{sc}, the open circuit voltage, V_{oc}, the maximum power, P_{max}, and the fill factor. Each parameter is shown with the standard deviation for 30 cells of each type.

B. Experimental Method

The discharge circuit is shown in Fig. 3. This represents a so-called inverted potential gradient, which is defined as the state in which the cover glass potential is more positive than the spacecraft chassis potential. During the substorm in geostationary orbit (GEO), the spacecraft potential becomes negative because of the incoming energetic electrons. The cover glass surface emits photoelectrons during the daytime and secondary electrons due to collision of the energetic electrons. When the electron emission is large enough, the potential of the cover glass surface becomes more positive than the spacecraft potential. In low Earth orbit (LEO), the potential of the spacecraft chassis where the solar array circuit's negative end is grounded is almost equal to the negative value of the solar array generation voltage due to high mobility of ionospheric electrons. In LEO, the cover glass potential is of the order of ion kinetic energy (5 eV) or electron temperature (less than 1 eV) and is negligible compared to the power generation voltage. Therefore, in LEO, the cover glass potential is more positive than the spacecraft chassis potential. A dc voltage power supply, V_b, simulates the spacecraft potential with respect to space. A capacitance, C_{ext}, simulates the capacitance of the dielectric parts on the solar array. C_{ext} supplies the primary discharge current. The voltage and current waveforms of the primary discharges are measured by a voltage probe and current probe, respectively.

Ideally, the lighted current–voltage characteristics (lighted IV) of a solar cell are necessary for checking the change in electrical performance due to a single primary discharge. To measure the lighted IV inside the vacuum chamber, the solar cell must be illuminated by light corresponding to the solar flux above Earth's atmosphere (AM0). But, at these fluxes, keeping the sample temperature constant inside the vacuum chamber is very difficult, and

Table 1 Electrical performance before the experiment in each solar cell

	I_{sc}, A	V_{oc}, V	P_{max}, W	Fill factor, %
MJ cell	0.45 ± 0.00	2.56 ± 0.01	0.97 ± 0.01	84.0 ± 0.0
Si w/ IBF cell	1.06 ± 0.01	0.61 ± 0.00	0.47 ± 0.01	71.7 ± 1.6
Si w/o IBF cell	1.07 ± 0.01	0.62 ± 0.00	0.47 ± 0.01	72.0 ± 2.0

such an illumination system attached to a vacuum chamber must be very complex. Because it is not realistic to measure the lighted IV in situ during a discharge experiment, the dark current–voltage characteristics (dark IV) were measured after each primary discharge to check the solar cell degradation. To measure the dark IV, the discharge circuit was disconnected, as shown in Fig. 3, and then connected a source meter to the solar cell electrodes. Figure 4 shows the typical dark IV of MJ cells. Here, to examine the change of dark IV of MJ cells during the degradation test, the current was defined at 1.5 V as I_{leak}. In the case of Si cells, I_{leak} is defined as the current value at 0.3 V.

The equivalent circuit of single-junction solar cells, such as Si cells, is shown in Fig. 5. Here, R_{sh} is the parallel resistance and R_s is the series resistance. Okumura et al. studied the degradation of Si cells in a simulated plasma environment in [3]. In their experiment, they measured the dark IV after each primary discharge. When the primary discharge parameter (such as peak current or energy) exceeded a certain threshold value, the I_{leak} gradually increased after each primary discharge. This was because the parallel resistance of the solar cells, R_{sh}, decreased after each primary discharge [3]. The simple equivalent circuit shown in Fig. 5 is only applied to single-junction solar cells. For MJ cells, it is not realistic to use this circuit. The equivalent circuit for MJ cells is more complicated but the degradation mechanism of MJ cells is fundamentally the same as that of Si cells, and MJ solar cell degradation can be discussed on the same basis.

Here, the increase in I_{leak} due to one discharge, dI_{leak}/dN_{arc}, is defined in Eq. (1). As stated in the Introduction, a primary discharge at the interconnector or bus bar does not cause solar cell degradation [4]. Therefore, N_{arc} does not include the number of arcs at the interconnector or bus bar. That is, N_{arc} is the number of primary discharges at the solar cell edge. Ideally, it is preferable to measure the dark IV after every primary discharge. However, when the discharge frequency is high, the primary discharge may occur several times before the bias was terminated to measure the dark IV. Therefore, dI_{leak}/dN_{arc} indicates the average value of the I_{leak} increase due to one primary discharge occurring on the surface of the solar cell. (In the case of an MJ cell, I_{leak} was normalized by an initial I_{leak} for each MJ cell. Therefore, the unit of dI_{leak}/dN_{arc} of an MJ cell is percent):

$$\frac{dI_{leak}}{dN_{arc}} = \frac{I_{leak_{after}} - I_{leak_{before}}}{N_{arc}} \qquad (1)$$
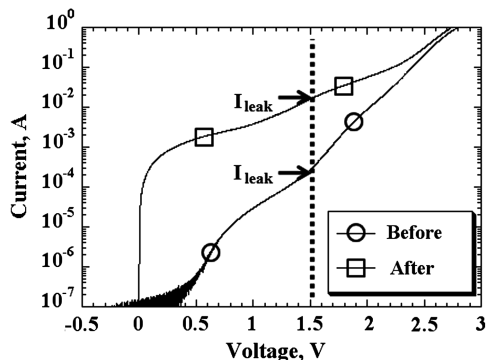

Fig. 4   Dark current–voltage characteristics of MJ cells before and after the experiment.
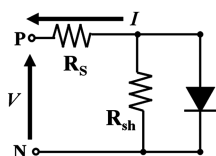

Fig. 5   Equivalent circuit of solar cells in dark condition.

C.   Measurement of Solar Cell Electrical Performance

The electrical performance of solar cells is obtained from the lighted current–voltage characteristics and lighted power–voltage characteristics (lighted PV). The lighted PV is calculated from the lighted IV. Figure 6 shows the lighted IV and lighted PV of MJ cells. I_{sc}, V_{oc}, and P_{max} are defined as shown in Fig. 6. The electrical performance of solar cells before and after the experiment in France, the United States, and Japan was measured at the Japan Aerospace Exploration Agency by using a solar simulator. The measurement error is lower than 1% (see Table 1). It is difficult to match the measurement conditions, such as temperature and light intensity, before and after the discharge experiment. Therefore, when the electrical performance before and after the experiment was compared, it should be noted that measurement uncertainty is typically 5%.

Here, the decrease rate of P_{max}, dP_{max}/dN_{arc}, is defined in Eq. (2) (as a percent). The decrease in P_{max} was normalized by the number of primary discharges at the solar cell, N_{arc}.

$$\frac{dP_{max}}{dN_{arc}} = \frac{(P_{max_{before}} - P_{max_{after}})}{P_{max_{before}} \times N_{arc}} \times 100 \qquad (2)$$

D.   Experimental Facility at the Kyushu Institute of Technology

The Kyushu Institute of Technology (KIT) has individual vacuum chambers to simulate the plasma environment in LEO (the LEO chamber) and GEO (the GEO chamber). The GEO chamber is 0.6 m in diameter and 0.9 m in length. It is equipped with an electron beam gun to generate high-energy electrons. During the experiment the acceleration voltage was set at 4 kV. To control the discharge frequency, the beam current density was changed to the order of 10 mA/m² on the sample surface. The current density is much higher than the electron flux at GEO to have an enough number of discharge in a limited experiment time. This current density is high compared to that found in the natural GEO environment (~10 uA/m²). Because the electron density of the primary discharge plasma is much higher than that of the electron beam, the high-current density of the electron beam was not taken into account. Because the bias voltage is set at −4.2 kV, only a small fraction associated with the high-energy tail of the electron beam for which the energy is centered at 4 kV can initially reach the surface. Once the cover glass surface reaches −4 kV, the majority of the electrons can reach and quickly charge the surface positively as the secondary electrons are effectively produced at the low-impact energy. The vacuum chamber pressure was approximately 3×10^{-3} Pa during the experiment.

The LEO chamber is 1 m in length and 1.2 m in diameter. It is equipped with an electron cyclotron resonance plasma source to generate a dense Xe plasma. With a 0.4 sccm gas flow, the plasma density is approximately 2×10^{12} m⁻³ and the electron temperature
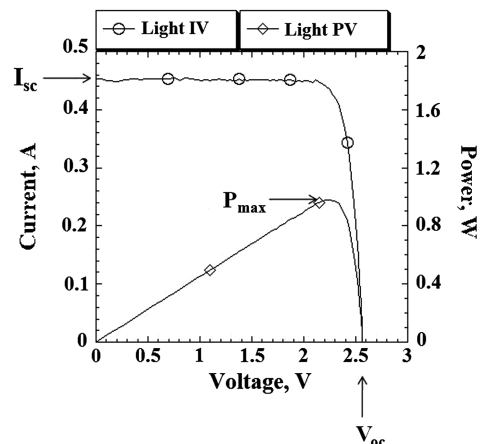

Fig. 6   The lighted current–voltage characteristics and the lighted power–voltage characteristics of MJ cells.

is approximately 1 eV [11]. Two types of turbomolecular pumps with different pumping rates were used to change the back pressure. During the experiment, the back pressure was 5.3×10^{-3} Pa with a 0.3 sccm gas flow and 2.1×10^{-3} Pa with 0.4 sccm. The plasma density and the electron temperature were kept constant at 2×10^{12} m^{-3} and 1 eV, respectively, although the vacuum chamber pressure was changing.

E. Experimental Facility at the NASA John H. Glenn Research Center at Lewis Field

The NASA John H. Glenn Research Center at Lewis Field uses a vacuum chamber, here called the GRC chamber, to simulate the plasma environment in LEO. The GRC chamber is 3 m in height and 2 m in diameter. It is equipped with a Kaufmann-type plasma source to generate a dense Xe plasma. The plasma density ranged from 0.4×10^{12} to 0.9×10^{12} m^{-3}. The electron temperature ranged from 1.1 to 1.4 eV. The vacuum chamber pressure during the experiment was approximately 7×10^{-3} Pa [10].

F. Experimental Facility of ONERA/Centre National d'Etudes Spatiales

ONERA uses a vacuum chamber, here called JONAS, to simulate the plasma environment in LEO. JONAS is 2 m in diameter and 3.4 m in length. It is equipped with a Kaufmann-type plasma source to generate the ions. The ion density is approximately 10^{12} m^{-3} and the drifting ion energy is approximately 20 eV with a 1 sccm argon gas flow. During the test, the vacuum chamber pressure was approximately 5×10^{-4} Pa [9]. The performance of all the experimental facilities is summarized in Table 2.

III. Results and Discussion

A. Definition of Primary Discharge Parameters

Figure 7 shows typical primary discharge voltage and current waveforms. The peak of the primary discharge current is defined as I_{peak}. T_{i1} and T_{i2} were defined as the time at which the current becomes 5% of I_{peak}. The primary discharge charge, Q_{arc}, is defined as

$$Q_{arc} = \int_{T_{i1}}^{T_{i2}} I(t)\, dt \qquad (3)$$

The duration of the primary discharge, T_{arc}, is defined as

$$T_{arc} = T_{i2} - T_{i1} \qquad (4)$$

To calculate the energy of the primary discharge, the voltage waveform was multiplied by the current waveform to obtain the power waveform. Figure 8 shows the power waveform of the primary discharge. The peak of the power waveform is defined as P_{peak}. T_{p1} and T_{p2} were defined as the time when the current becomes 5% of P_{peak}. The energy of the primary discharge, W_{arc}, is defined as

$$W_{arc_1} = \int_{T_{p1}}^{T_{p2}} V(t) \times I(t)\, dt \qquad (5)$$

In the case of the experiment in a high-energy electron environment, that is, the GEO chamber, a high-voltage probe was used to measure the change in V_b. Because the voltage probe signal was attenuated, the measured voltage waveform was not used to calculate the power waveform. Therefore, only the current waveform was used
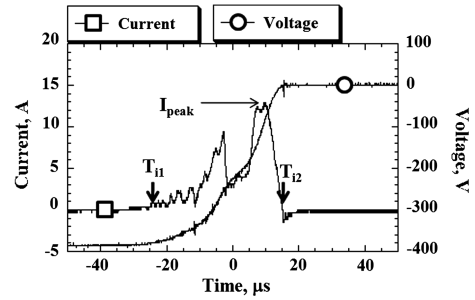
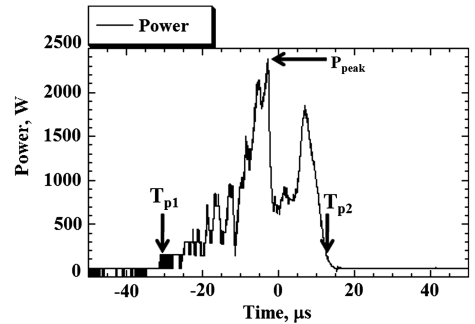**Fig. 7 Primary discharge current and voltage waveform.**

Fig. 8 Power waveform of primary discharge.

to calculate the energy, as shown in Eq. (6). As the external capacitance, C_{ext}, is much larger than the capacitance of cover glass (approximately 1 nF or less), the capacitance of cover glass in Eq. (6) was ignored:

$$W_{arc_2} = \frac{Q_{arc}^2}{2C_{ext}} \qquad (6)$$

B. Comparison of Primary Discharge Current Waveforms

As shown in Table 2, the vacuum chamber pressure, plasma density, and electron temperature are different between the LEO chamber, the GRC chamber, and JONAS. Figures 9 and 10 show examples of primary discharge current waveforms measured at the different facilities. In Fig. 9, the primary discharge current waveform in the GEO chamber is also shown. The discharge experiments shown in Figs. 9 and 10 were carried out on MJ cells. Table 3 shows the vacuum chamber pressure, C_{ext}, V_b, T_{arc}, and Q_{arc}. The time T_{arc} and the charge Q_{arc} are the average and the standard deviations over the number of discharges listed in the bottom row. The Q_{arc} was almost same among the different facilities. However, the primary discharge current waveforms were different.

In our experiment, the capacitance, C_{ext}, is the major current supply for electrostatic discharge, as explained in Sec. III.A. There is no apparent circuit element to limit the current from the capacitance. Therefore, the charge from the capacitance is instantaneously released after the discharge inception. In the real solar array, the solar cell cover glass is the major current source of the electrostatic discharge. A flashover plasma expanding with a finite velocity releases the cover glass charge, giving a longer duration than seen in the present experiment. The purposes of the present paper are to

Table 2 Summary of experimental facilities

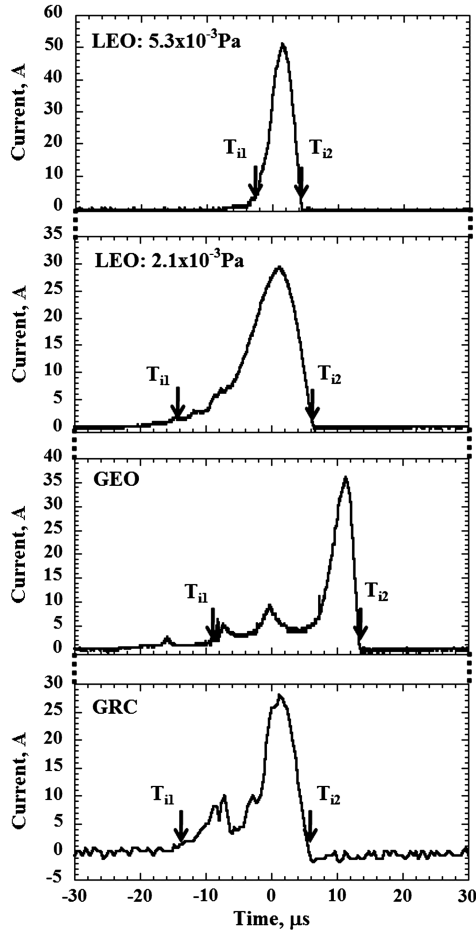|	LEO	JONAS	GRC	GEO	
Charging source		Plasma		High-energy electron beam	
Size	1 m × 1.2 m	2 m × 3.4 m	3 m × 2 m	0.6 m × 0.9 m	
Pressure, Pa	2.1×10^{-3} or 5.3×10^{-3}	5×10^{-4}	7×10^{-3}	3×10^{-3}	
Plasma density	1×10^{12} m^{-3}	10^{12} m^{-3}	0.4×10^{12} m^{-3} to 0.9×10^{12} m^{-3}	Electron energy	4 keV
Electron temperature	1 eV	0.1–0.2 eV	1.1–1.4 eV	Current density	Order of 10 μA/m^2

Fig. 9 Typical primary discharge waveform in the LEO chamber, the GEO chamber, and the GRC chamber.
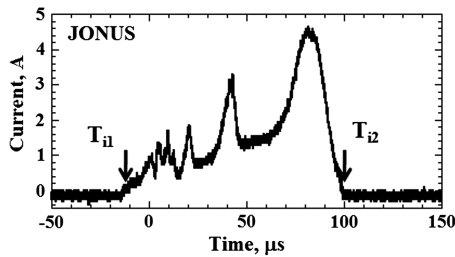

Fig. 10 Typical primary discharge waveform in JONAS.

confirm the solar cell degradation in three different places using a simple circuit setup and to characterize the degradation.

C. Discharge Experiment on Multijunction Cells

Table 4 shows the experimental conditions for MJ cells. Figures 11–13 show the relationship between dI_{leak}/N_{arc} and I_{peak}, dI_{leak}/N_{arc} and T_{arc}, and dI_{leak}/N_{arc} and W_{arc}, respectively. To

investigate the dependence of the discharge parameter on dI_{leak}/N_{arc}, the first-order regression curve was applied to the data (Figs. 11–13). The regression curves of I_{peak}, T_{arc}, W_{arc} against dI_{leak}/N_{arc} are given by Eqs. (7–9) with coefficient of correlation, R:

$$dI_{leak}/N_{arc} = 2.6 \times I_{peak} + 7.6, \qquad R = 0.32 \qquad (7)$$

$$dI_{leak}/N_{arc} = -3.3 \times T_{arc} + 59.0, \qquad R = 0.11 \qquad (8)$$

$$dI_{leak}/N_{arc} = 539 \times W_{arc} + 13, \qquad R = 0.42 \qquad (9)$$

The coefficient of correlation ranges from 0 to 1; $R = 1$ is the best correlation. The dI_{leak}/N_{arc} is positively proportional to the I_{peak} and W_{arc}. Contrary to I_{peak} and W_{arc}, dI_{leak}/N_{arc} is negatively proportional to T_{arc}. In addition, the coefficient of correlation is the worst among Eqs. (7–9). This fact suggests that the I_{peak} and W_{arc} are the dominant discharge parameters on solar cell degradation and not T_{arc}.

Figures 14–16 show the relationship between dP_{max}/N_{arc} and I_{peak}, dP_{max}/N_{arc} and T_{arc}, and dP_{max}/N_{arc} and W_{arc}, respectively. Based on the results of the discharge experiment, the MJ cells suffered degradation in all of the facilities. Therefore, solar cell degradation is not peculiar to a specific facility. Table 5 shows the minimum primary discharge conditions for degradation on MJ cells in terms of I_{peak} and W_{arc}. At all three facilities, the degradation was observed even with the minimum values of C_{ext} and V_b, that is, the minimum discharge energy. Because the starting parameters of the experiments were different, the values listed in Table 5 are different. Here, "before I_{leak}" and "after I_{leak}" indicate the I_{leak} before and after the number of discharges. N_{arc} is listed in the bottom row of the table.

Figures 14–16 show that dP_{max}/N_{arc} increases with higher I_{peak} and higher W_{arc}. The tendency shown in Figs. 14–16 is similar to the tendency shown in Figs. 11–13. According to Figs. 14 and 16, when I_{peak} and W_{arc} are sufficiently high, MJ cells may lose several tens of percent of power generation even from one primary discharge. Even in the case of a primary discharge with several millijoules of W_{arc} and several amps of I_{peak}, repetitive primary discharges may cause serious degradation to MJ cells. Based on the results of the discharge experiment on MJ cells, I_{peak} and W_{arc} are the dominant parameters to characterize the degradation.

In the discharge experiment, C_{ext} and V_b determine W_{arc}. The resistance of the primary discharge circuit and C_{ext} determine I_{peak}. Here, the resistance of the primary discharge circuit is the resistance of the discharge circuit including the cable harness and the resistance associated with the primary discharge. As mentioned earlier, C_{ext} simulates the capacitance of the solar array surface. The results of the round-robin discharge experiment on MJ cells warn us that an excessive C_{ext} may cause excessive degradation, which is unrealistic. The value of C_{ext} should be selected to be representative of the flight condition as much as possible.

D. Discharge Experiment on Si With and Without Integrated Bypass Function Cells

Table 6 shows the experimental conditions on Si with and without IBF cells. Figures 17–19 show the relationship between dI_{leak}/N_{arc} and I_{peak}, dI_{leak}/N_{arc} and T_{arc}, and dI_{leak}/N_{arc} and W_{arc}, respectively. dI_{leak}/N_{arc} does not correlate with I_{peak}, T_{arc}, and W_{arc} in Figs. 17–19. dI_{leak}/N_{arc} is mainly on the order of 10^{-5} A or 10^{-3} A. The

Table 3 Primary arc parameter in different facility

	LEO		GEO	GRC	JONUS
Pressure, Pa	5.3×10^{-3}	2.1×10^{-3}	3×10^{-3}	7×10^{-3}	5×10^{-4}
C_{ext}, F	5×10^{-4}	5×10^{-4}	6.5×10^{-5}	4.7×10^{-4}	5×10^{-4}
V_b, V	-400	-600	-4200	-400	-630
T_{arc}, μs	8.3 ± 0.7	16.5 ± 2.6	23.3 ± 8.7	18.9 ± 2.5	86.2 ± 2.4
Q_{arc}, mC	0.21 ± 0.08	0.19 ± 0.01	0.20 ± 0.01	0.18 ± 0.01	0.26 ± 0.05
N_{arc}	16	25	5	20	20

Table 4   Experimental conditions for MJ cell

	LEO chamber	GEO chamber	GRC chamber	JONAS
Number of MJ cells	9	5	6	8
Range of C_{ext}	5×10^{-8} F to 5×10^{-7} F	2.5×10^{-10} F to 1×10^{-7} F	7.5×10^{-8} F to 1×10^{-6} F	2×10^{-7} F to 1×10^{-6} F
Pressure, Pa	5.3×10^{-3}	3.0×10^{-3}	7.0×10^{-3}	5.0×10^{-4}

degradation mode of solar cells is categorized into two types (see Fig. 20). The primary discharge creates a discharge track on the solar cells. When the discharge track locally destroys the P–N junction of the solar cells, I_{leak} does not increase significantly. In Fig. 20, this type of discharge track is defined as type 2. In this case, dI_{leak}/N_{arc} is on the order of 10^{-5} A. The case in which the discharge track destroys the P–N junction and shorts the N electrode and P electrode or the P layer is defined as type 1 in Fig. 20. The resistance in the type 1 case is smaller than in the type 2 case. In the type 1 case, dI_{leak}/N_{arc} is on the order of 10^{-3} A. In [5], the discharge track defined as type 1 is studied in detail.

dI_{leak}/N_{arc} is on the order of 10^{-2} A at maximum in the cases of Si with and without IBF cells. The primary discharge causes damage on the solar cell edge. Because the IBF exists in the Si bulk, the IBF does not affect dI_{leak}/dN_{arc}.

Earlier, the relationship between the primary discharge parameters and dI_{leak}/N_{arc} was discussed. Next, the relationship between dI_{leak}/N_{arc} and the change in electrical performance will be discussed. The relationship between I_{leak} after the experiment and the change of P_{max} before and after the experiment, ΔP_{max}, is shown in Fig. 21 for all the three types of cells tested. ΔP_{max} is defined by Eq. (10). dP_{max}/N_{arc} stands for the decrease of P_{max} due to one primary discharge. However, ΔP_{max} does not depend on the number of primary discharges, that is, ΔP_{max} (in percent) is the actual power decrease before and after the experiment:
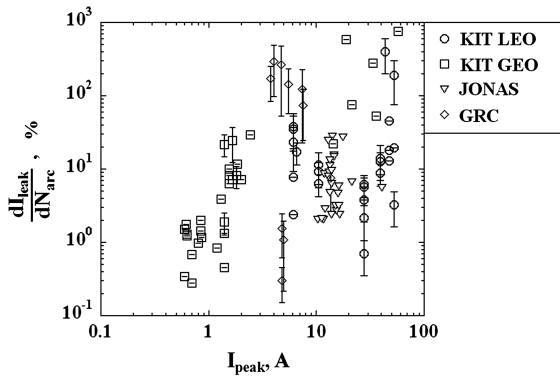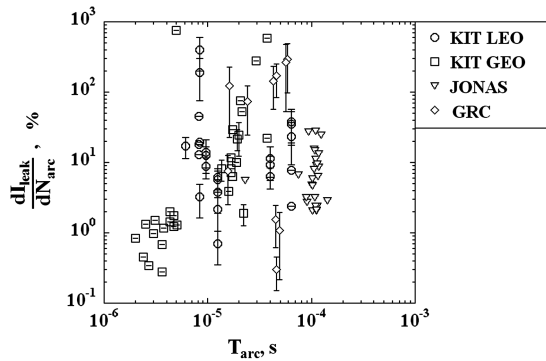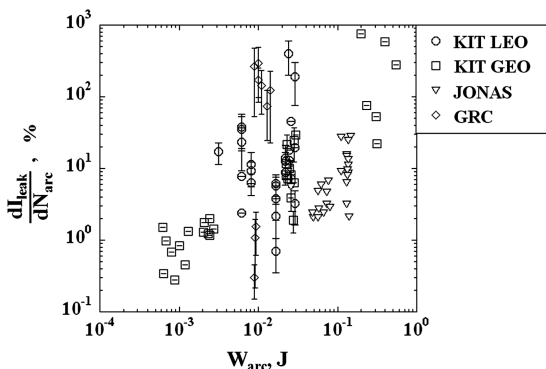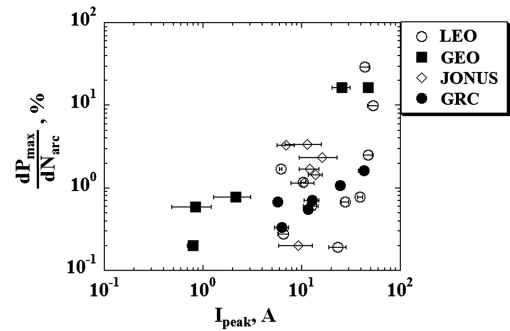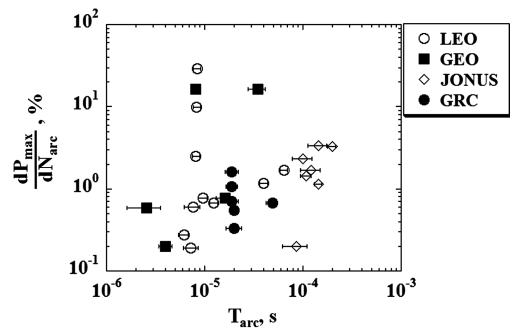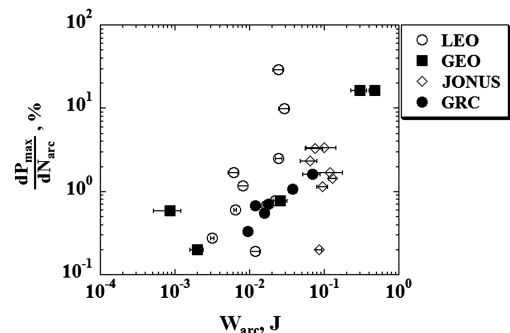

Fig. 11   Relationship between dI_{leak} and I_{peak} on MJ cells.

Fig. 12   Relationship between dI_{leak} and T_{arc} on MJ cells.

Fig. 13   Relationship between dI_{leak} and W_{arc} on MJ cells.

Fig. 14   Relationship between dP_{max} and I_{peak} on MJ cells.

Fig. 15   Relationship between dP_{max} and T_{arc} on MJ cells.

Fig. 16   Relationship between dP_{max} and W_{arc} on MJ cells.

Table 5   Minimum parameter for degradation on MJ cell

	LEO chamber	GEO chamber	GRC chamber	JONUS
I_{peak}, A	6.5 ± 0.8	0.8 ± 0.1	3.9 ± 0.7	6.9 ± 1.4
T_{arc}, μs	6.1 ± 0.7	4.0 ± 0.6	18.0 ± 2.3	198 ± 18
W_{arc}, mJ	3.1 ± 0.2	1.9 ± 0.4	7.3 ± 1.1	75 ± 19
Before: I_{leak}, A	1.88×10^{-4}	1.18×10^{-3}	7.30×10^{-6}	2.25×10^{-4}
After: I_{leak}, A	4.45×10^{-3}	9.03×10^{-3}	9.60×10^{-4}	1.59×10^{-2}
dP_{max}/N_{arc}, %	0.6	0.6	0.7	1.7
N_{arc}	11	21	20	12

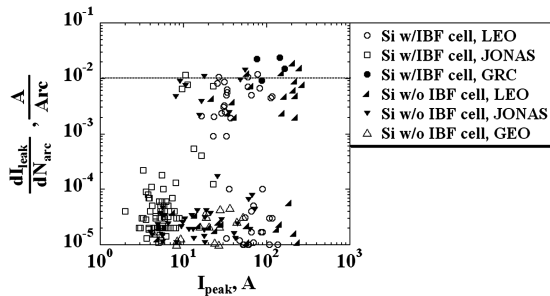**Table 6   Experimental conditions of Si with and without IBF cells**

Facility	Solar cell type	No. of samples	Range of C_{ext}	Pressure, Pa
LEO	Si w/ IBF cell	8	5×10^{-8} F to 1.9×10^{-6} F	2.1×10^{-3} or 5.3×10^{-3}
	Si w/o IBF cell	7	5×10^{-8} F to 5×10^{-6} F	
GRC	Si w/ IBF cell	5	1.5×10^{-7} F to 2×10^{-6} F	7.0×10^{-3}
	Si w/o IBF cell	3	1.5×10^{-7} F to 2×10^{-6} F	
JONAS	Si w/ IBF cell	7	2×10^{-7} F to 1×10^{-6} F	5.0×10^{-4}
	Si w/o IBF cell	10	2×10^{-7} F to 1×10^{-6} F	
GEO	Si w/o IBF cell	2	4×10^{-9} F to 1×10^{-7} F	3.0×10^{-3}

Table 7   Minimum discharge parameters for having I_{leak} increase beyond 10^{-2} A for silicon solar cells

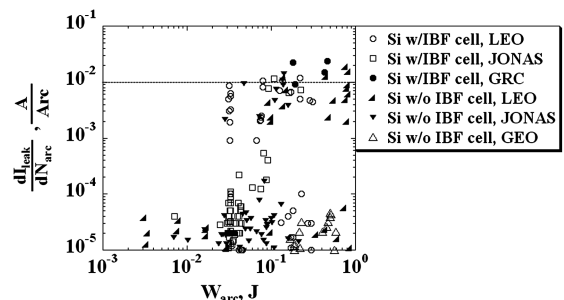|		I_{peak}, A	T_{arc}, s	W_{arc}, J	dI_{leak}/N_{arc}, A	ΔP_{max}, %
Si w/ IBF cell	LEO	26.6	2.83×10^{-5}	7.90×10^{-2}	1.04×10^{-2}	-1.1
	JONAS	10.6	8.18×10^{-5}	1.08×10^{-1}	1.16×10^{-2}	1.3
Si w/o IBF cell	LEO	59.0	2.70×10^{-5}	1.40×10^{-1}	1.22×10^{-2}	6.6
	JONAS	17.9	8.58×10^{-5}	1.36×10^{-1}	1.11×10^{-2}	0.8

$$\Delta P_{max} = \frac{(P_{max_{before}} - P_{max_{after}})}{P_{max_{before}}} \times 100 \qquad (10)$$

In the case of MJ cells, ΔP_{max} increases with increasing I_{leak} after the experiment. From Fig. 21, once I_{leak} exceeds 10^{-2} A, P_{max}

decreases beyond the measurement error. Contrary to the MJ cells, Si with and without IBF cells did not suffer significant degradation. However, when I_{leak} is more than 10^{-2} A, ΔP_{max} is higher than the measurement error for some Si cells. Therefore, the solar cell degradation when I_{leak} exceeds 10^{-2} A can be evaluated in the discharge experiment. The advantage of the evaluation of solar cell degradation from the dark IV is that the experimental system and procedure is much simpler than the case in which the lighted IV was measured. The maximum I_{leak} after the experiment with Si with and without IBF cells is 2×10^{-2} A and 3×10^{-2} A, respectively. There were several primary discharges that caused I_{leak} to increase by more than 10^{-2} A, as shown in Figs. 17–19. The minimum primary discharge conditions of those primary discharges giving $I_{leak} > 10^{-2}$ A are shown in Table 7. Considering the flashover current in the ground experiment as compared to that in orbit, the energy of the primary discharge is expected to range from several to several hundred millijoules in orbit. Additionally, it cannot be denied that repetitive arcs can cause more serious degradation on Si cells.

The maximum I_{leak} after the experiment with the Si with and without IBF cells is in the order of 10^{-2} A. However, the maximum I_{leak} after the experiment with MJ cells is in the order of 10^{-2} A.

Fig. 17   Relationship between dI_{leak} and I_{peak} on Si with and without IBF cells.
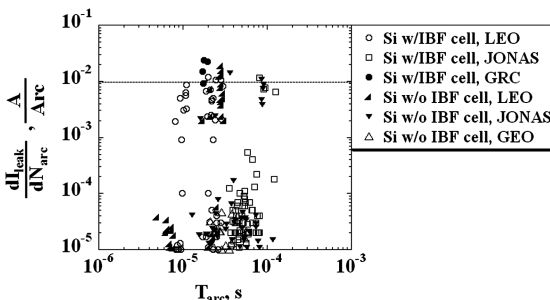
Fig. 18   Relationship between dI_{leak} and T_{arc} on Si with and without IBF cells.

Fig. 19   Relationship between dI_{leak} and W_{arc} on Si with and without IBF cells.
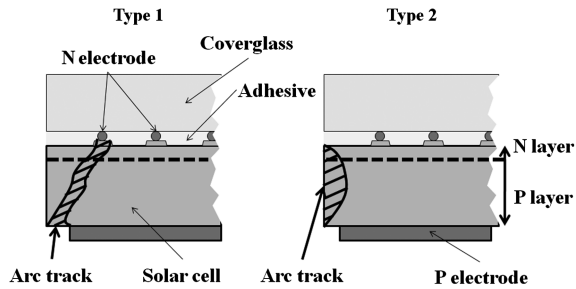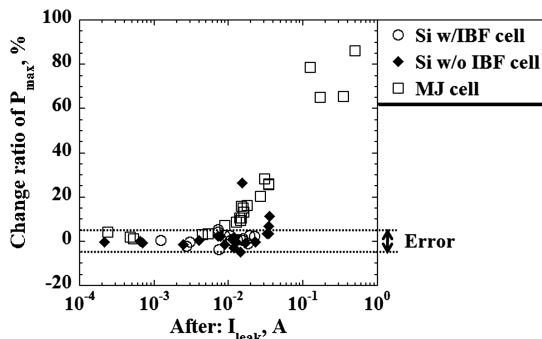
Fig. 20 Discharge tracking model.

Fig. 21 Relationship between the decrease in solar cell electrical output and I_{leak} after each test.

Figure 21 shows that I_{leak} of the Si cells is obviously not increasing like that of MJ cells. This fact supports the suggestion that the Si cells are more robust than MJ cells against the primary discharge. The reason for this should be the subject of a future examination.

IV. Conclusions

To establish an international standard for solar array electrostatic discharge tests, an international round-robin experiment was carried out regarding solar cell degradation due to repeated primary discharges in France (ONERA/Centre National d'Etudes Spatiales), the United States (NASA John H. Glenn Research Center at Lewis Field), and Japan (Kyushu Institute of Technology). The purpose of the round-robin experiment was to confirm that the solar cell degradation is possible. In the experiment, a common test circuit and a common experiment procedure were employed.

The use of different vacuum chambers and charging methods among the different institutions gave various discharge waveforms. Although the waveforms were different, the solar cell degraded in all the chambers that were tested was confirmed. The leak current, defined as a forward direction current when biased to 1.5 V for MJ cells and 0.3 V for Si cells in a dark condition, can be used as an indicator of the solar cell degradation. There was a correlation between the increase of the leak current and the degradation of solar cell electrical output, that is, P_{max}. For both MJ and Si cells, a degradation of P_{max} beyond the measurement uncertainty was observed when the leak current exceeded 0.01 A. Therefore, by monitoring the dark IV characteristics during the solar array ESD test, it was possible to identify when the test specimen degraded without carrying out an expensive and difficult in situ lighted IV measurement.

In the case of MJ cells, solar cell degradation worsened as the peak current and the energy increased. In the case of Si cells, the integrated bypass-diode function did not affect the degradation. In the case of Si cells, although there was little correlation between the primary discharge parameters such as the peak current or the energy and the increase of the leak current, there were two ways in which the leak current increased. These two ways probably depended on whether an discharge track short circuited the P and N electrodes by penetrating through a solar cell or formed a thin layer of leak current path along the surface of solar cell. After performing experiments with the same primary discharge parameters, Si solar cells degraded less than MJ solar cells.

As it is now recognized that a solar cell degrades due to primary discharge, the next issue to be examined is how this should be taken into account in the design of spacecraft power systems, besides the obvious issue of mitigating the primary discharge inception itself. If the discharge current waveform on-orbit and how many primary discharges occur during the spacecraft's lifetime are known, how much power will be lost at the end of the spacecraft's lifetime can be statistically estimated. To do so, a database is needed that shows how a solar cell degrades for different sets of primary discharge parameters, models of discharge waveforms, and the number of primary discharges on-orbit. It would also be necessary to examine the degradation characteristics of new types of solar cells, such as thin-film solar cells, in the near future.

Solar cell degradation due to radiation has been widely recognized and verified by various on-orbit measurements. The degradation due to primary discharge has been confirmed only in laboratory experiments. As mentioned in the Introduction, the primary discharge locally injects thermal energy into the solar cell. Therefore, there should not be a significant difference between the effect of arcs in space and on the ground. It is still strongly recommended to demonstrate that primary discharge-induced degradation occurs in orbit. Demonstration via a simple on-orbit experiment is possible. What is needed is a discharge detection device, a discharge waveform measurement device, and an IV curve measurement device. An effort to find a flight opportunity for such an on-orbit experiment should be started as soon as possible.

Acknowledgments

References

[1] Toyoda, K., Matsumoto, T., Cho, M., Nozaki, Y., and Takahashi, M., "Power Reduction of Solar Arrays Due to Arcing Under Simulated GEO Environment," *Journal of Spacecraft and Rockets*, Vol. 41, No. 5, 2004, pp. 854–861.
doi:10.2514/1.13103

[2] Toyoda, K., Okumura, T., Cho, M., Nozaki, Y., and Takashi, M., "Degradation of High Voltage Solar Array Due to Arcing in LEO Plasma Environment," *Journal of Spacecraft and Rockets*, Vol. 42, No. 5, 2005, pp. 947–953.
doi:10.2514/1.11602

[3] Okumura, T., Masui, H., Toyoda, K., Imaizumi, M., and Cho, M., "Degradation of Electric Performance Due to Electrostatic Discharge on Silicon Solar Cell for Space," *Journal of the Japan Society for Aeronautical and Space Sciences*, Vol. 55, No. 647, 2007, pp. 590–596.
doi:10.2322/jjsass.55.590

[4] Okumura, T., Hosoda, S., Kim, J., Toyoda, K., and Cho, M., "Degradation of High Voltage Solar Array Due to Arcing in LEO Plasma Environment," Japan Aerospace Exploration Agency Paper 2004-s-06, June 2004.

[5] Clevenger, B., Hise, L., Newman, N., Aiken, D., and Sharps, P., "Evaluation of ESD Susceptibility of Solar Cells with a Monolithic Diode," *Conference Record of the 2006 IEEE 4th World Conference on Photovoltaic Energy*, Vol. 2, Inst. of Electrical and Electronics Engineers. New York, pp. 1931–1934.

[6] Hastings, D., and Garrett, H., *Spacecraft Environment Interactions*, Cambridge Univ. Press, New York, 1996, pp. 142–198.

[7] Cho, M., "Status of ISO Standardization Efforts of Solar Panel ESD Test Methods," *10th Spacecraft Charging Technology Conference on Disk [CD-ROM]*, Centre National d'Etudes Spatiales, Toulose, France, June 2007.

[8] Okumura, T., Ninomiya, S., Masui, H., Toyoda, K., Imaizumi, M., and
     Cho, M., "Solar Cell Degradation Due to ESD for International
     Standardization of Solar Array ESD Test," *10th Spacecraft Charging
     Technology Conference*, Centre National d'Etudes Spatiales, Toulose,
     France, June 2007.
[9] Mateo-Velez, J., Inguimbert, V., Roussel, J., Sarrail, D., Levy, L.,
     Boulay, F., Laffont, E., and Payan, D., "ESDs on Solar Cells –
     Degradation, Modeling, and Importance of the Test Setup," *IEEE
     Transactions on Plasma Science*, Vol. 36, No. 5, Oct. 2008, pp. 2395–
     2403.
     doi:10.1109/TPS.2008.2001835

[10] Vayner, B., Ferguson, D., and Galofaro, J., "Detrimental Effect of
     Arcing on Solar Array Surfaces," *10th Spacecraft Charging
     Technology Conference on Disk [CD-ROM]*, Centre National d'Etudes
     Spatiales, Toulose, France, June 2007.
[11] Hayashi, H., Saionji, A., Toyoda, K., Cho, M., and Kuninaka, H.,
     "Development of Plasma Interaction Acceleration Test Facility for
     Study on Space Material Deterioration," Japan Aerospace Exploration
     Agency Paper 2002-b-28, 2002.

A. Ketsdever
Associate Editor